JOURNAL OF PROPULSION AND POWER
Vol. 18, No. 5, September–October 2002

High Strain-Rate Constitutive Models for Solid Rocket Propellants

Sook-Ying Ho*
Defence Science and Technology Organisation, Edinburgh, South Australia 5108, Australia

A constitutive model that incorporates mechanical damage and nonlinear viscoelastic material response for solid composite rocket propellants has been developed for high strain-rate impact loading conditions. The numerical constants in this model could be related to the physics of the propellant and were obtained by nonlinear least-squares fitting of the data obtained from Hopkinson Bar experiments in the strain-rate range from 10^3 to 10^4 s^{-1}. Damage was taken into account using an approach based on correcting the viscoelastic function with a stress softening function. A simple method for calibrating the stress softening function using the recoverable strain energy density has been developed. This energy-based approach has the advantage of being able to capture damage more adequately and allows for bulk inelastic behavior. Predictions of the stress response of two different composite propellants for different loading conditions (temperature and strain rate) and histories (and, therefore, different damage levels) were made using the constitutive model. Good agreement between the predicted and experimentally measured stresses for strain levels up to 30–40% was obtained. The model was able to predict the stress response quite reasonably outside the temperature range used to develop the constitutive equation, but inside the range of the reduced strain-rate, indicating the validity of the time–temperature superposition principle for high strain-rate conditions. The model was also able to reproduce quite well the mechanical deformation (both in magnitude and shape of the stress–strain curve) of predamaged propellants.

Nomenclature

a_T	=	time–temperature shift factor
$\lvert d\varepsilon/dt \rvert$	=	absolute strain rate
E	=	modulus in initial linear elastic region of stress–strain curve
f	=	viscoelastic stress
G''	=	dynamic shear loss modulus
g	=	stress softening function
H_r	=	hysteresis ratio
m	=	exponent for strain softening/hardening
n	=	exponent for strain-rate dependence
T	=	temperature
T_g	=	glass transition temperature
T_0	=	reference temperature
W_i	=	input strain energy density
W_{rc}	=	recoverable strain energy density
ε	=	strain
$\dot{\varepsilon}$	=	strain rate
η	=	"pseudo," or artificial, viscosity
σ	=	stress

Introduction

CONSTITUTIVE models that incorporate cumulative damage and can take into account temperature and strain-rate dependence are key to the development of improved and more accurate capabilities for predicting the response of munitions to impact stimuli, ranging from accidental handling impacts to projectile/fragment attack. The benefits of the improved prediction capabilities include reduced full-scale hazard testing, resulting in substantial cost savings and increased confidence in the safety of munitions.

Received 16 November 2001; revision received 5 April 2002; accepted for publication 5 June 2002.

*Principal Research Scientist, Weapons Systems Division, Aeronautical and Maritime Research Laboratory.

Under certain conditions, solid rocket motors can detonate at significantly lower impact stresses than required for prompt shock initiation. A current deficiency in modeling delayed detonation (XDT) and deflagration-to-detonation reactions in rocket motors is the lack of physics-based material and damage models. Deformation/damage plays an important role in hot-spot initiation,[1–3] that is, localization of energy in shear bands, microcracks, etc., and in the rarefaction (resulting in internal tensile damage), followed by the recompaction mechanism,[4] generally believed to be responsible for XDT. Hence, to model accurately the structural response of rocket motors under dynamic loading conditions appropriate to XDT, high strain-rate constitutive models that can account for the effect of temperature, loading history, and damage evolution are required.

Solid rocket propellants exhibit nonlinear viscoelastic (NLVE) behavior,[5–8] that is, their deformation/fracture properties are highly strain-rate and temperature dependent, and only a portion of the applied strain energy is recoverable. The material nonlinearity of solid propellant behavior is due in large to damage processes, such as volume change/dewetting of the oxidizer particles from the polymeric binder and, to a lesser extent, thermomechanical coupling and modulus strain sensitivity. It is also well known that partial recovery occurs in damaged composite propellants when they are left in an unstrained condition over a period of time. At present, there is a lack of suitable material models that can adequately describe cumulative damage under high strain-rate loading conditions. In the low strain-rate regime, two distinct methods have been used to treat damage in NLVE materials. First, damage is based on some continuum variables, for example, time to failure and strength, described by some failure criteria such as linear and nonlinear cumulative damage and Lebesque norm of stress models. However, recent studies[9] indicate that these models underpredict the damage. (For example, failure criteria based on stress or strain capabilities alone could not predict the time to failure.) The ultimate strain or strain-energy density capability may be a more accurate measure of damage. Second, a damage function is utilized as an implicit component of the NLVE constitutive theory to modify the stress response during repeated loading cycles.

The objective of the present study is to develop a high strain-rate constitutive model that incorporates mechanical damage and temperature and strain-rate dependence. This model has to be able to predict the complex nonlinear viscoelastic response of solid rocket

propellants under high strain-rate loading and can be implemented into a finite element code. The features of this model include the following: 1) The numerical parameters of the model can be related to the physics of the propellant and obtained by nonlinear regression analysis of the experimental data from the modified Hopkinson Bar (see Refs. 10–12) at strain rates in the range 10^3–10^4 s^{-1}. 2) Temperature and strain-rate dependence is handled using the time–temperature superposition principle. 3) Damage is incorporated in the constitutive equation using the "stress correction" approach of Swanson and Christensen[13] (also see Ref. 14), where a stress softening function is used to correct the stress response. 4) A continuum energy-based approach is used to determine the stress softening data from simple loading experiments. A suitable function that can account for the effect of different loading variables such as strain rate to fit the stress softening data is determined.

The response predicted by the models for two different composite rocket propellants is compared with the experimental data for different loading conditions. The ultimate aim is to couple the models for propellant deformation response with a reaction (ignition and growth) model to predict hot spots and ignition resulting from cumulative damage.

Experimental

Two different solid composite rocket propellants were used for this study: HTPB/AP [17:83 wt% of hydroxy-terminated polybutadiene binder and ammonium perchlorate (AP) oxidizer] and PPG/AP (18:82 wt% polypropyleneglycol binder and AP oxidizer). The propellants were machined into 8 × 8 mm cylindrical pellets for the modified Hopkinson Bar test.

Damage was induced in the propellant specimens by either 1) constant stress experiments using a Rheometrics Solid Analyser, Model RSA2 or 2) monotonic constant strain-rate tests.

Modified Hopkinson Bar

A modified Hopkinson Bar was used to assess the high strain-rate (10^3–10^4 s^{-1}) behavior of the undamaged and predamaged propellant specimens. This test has been described in detail in previous papers.[11,12] Experiments were conducted in duplicates at three different velocities in the temperature range from −50 to +60°C. The ends of the specimen were lubricated to minimize the effects of friction. The specimen geometry was chosen to minimize frictional effects at the specimen–bar interfaces and inertial stresses (that would result in nonuniform stress distribution).

For the temperature dependence studies, the specimens were conditioned for at least 1 h at the required temperature, quickly removed, and fixed to the output stationary bar (connected to strain gauges to measure applied loads) by grease. The time elapsed from removal of the specimen from temperature conditioning until testing was 2–3 min. A moving input bar was then fired (using a commercial ramset gun) at the specimen, which was compressed between the two bars. The load-displacement data were collected using a four-channel digital oscilloscope and the data analyzed as described earlier.[3,11,12]

The predamaged specimens were tested immediately after damage was induced to minimize the effect of rehealing.[8] All experiments on the predamaged propellants were conducted at 25°C.

Damage Characterization

Constant stress (creep) tests/experiments were conducted at ambient temperature on the Rheometrics Solid Analyser using a cylindrical/tension fixture for 8-mm-diam cylindrical specimens at a stress level of 0.5 MPa. The strain rate was ≈10^{-6} s^{-1}. The strain was monitored as a function of time, and the test was stopped when failure was observed to occur or when a given time limit was reached, to induce different levels of damage in the specimens.

Results and Discussion

Development of High Strain-Rate Constitutive Models

The stress–strain curves at various temperatures for the HTPB/AP propellant are shown in Fig. 1. Interpretation of the deformation and

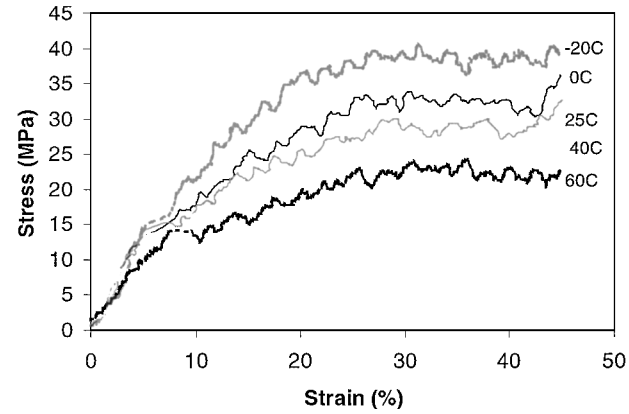

Fig. 1a Stress-strain curves for HTPB/AP propellant at various temperatures (mean strain rate ≈3200 s^{-1}).

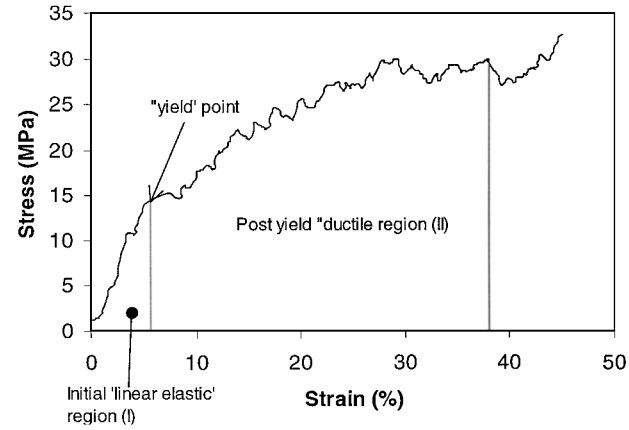

Fig. 1b Schematic stress–strain curve defining the regions where the various fracture deformation processes occur.

fracture processes that occur in the different regions of the stress–strain curve from the Hopkinson Bar test has been discussed in detail previously,[3,7,11,12] but, for the sake of clarity, will be briefly outlined here. On impact of the specimen, various processes occur in the different regions of the observed stress–strain curve. (Figure 1a shows the deformation up to 30–40% strain.) Yielding and formation of voids/microcracks occur in region 1, the initial linear elastic region, as evidenced by scanning electron microscopy examinations.[11] Viscoelastic/plastic deformation, further crack propagation, and other secondary deformation mechanisms occur in region 2. Photography experiments of the impact event showed that the propellant is still intact in this region.[3] Yielding occurred in the high strain-rate compression tests at all temperatures in this study (from −20 to +60°C). Above the brittle-to-ductile transition temperature, this propellant undergoes extensive plastic deformation followed by ductile and/or shear failure.

The stress–strain data were fitted to a multivariate function using the Levenberg–Marquardt nonlinear least-squares fitting technique to search for coefficients that minimize χ^2 (discrepancy between the function and raw data). At a given temperature, the viscoelastic constitutive equation has the form

$$\sigma = E\varepsilon^m + \eta\left|\frac{d\varepsilon}{dt}\right|^n \tag{1}$$

where σ is in megapascal, ε is in percent, and $|d\varepsilon/dt|$ is in s^{-1} (calculated from the true strain and time t). The coefficients in the fitted function can be interpreted from the Nomenclature. The first term in this equation models the elastic/plastic deformation. The second term is the viscoelastic or strain-rate effect, which raises the stress level for a given strain by a factor determined by the strain-rate sensitivity of the material.

Table 1 Fit coefficients for stress as a function of strain and strain rate [Eq. (1)] for HTPB/AP propellant at various temperatures; mean strain rate ≈3200 s^{-1}

Temperature, °C	$E \pm 1\sigma$, MPa	$m \pm 1\sigma$	$\lvert\eta\rvert \pm 1\sigma$, MPa s^{-1}	$n \pm 1\sigma$
−20	9.1 ± 0.4	0.41 ± 0.01	0.01 ± 0.06	0.4 ± 0.8
0	7.2 ± 0.2	0.388 ± 0.009	0.02 ± 0.2	0.4 ± 1
25	5.2 ± 0.1	0.517 ± 0.008	0.01 ± 0.02	0.8 ± 0.8
40	4.8 ± 0.2	0.52 ± 0.01	0.01 ± 0.03	0.9 ± 1
60	5.0 ± 0.1	0.434 ± 0.008	0.01 ± 0.05	0.6 ± 0.9

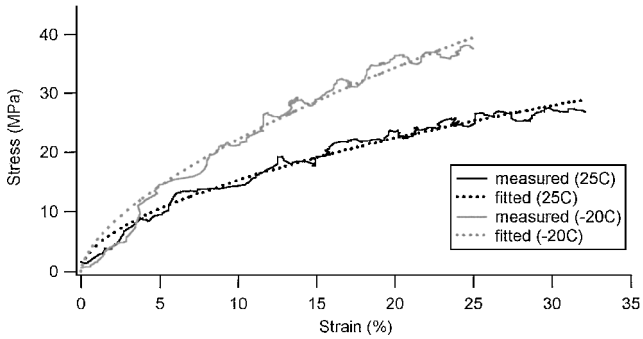

Fig. 2 Comparison between fitted and experimental stress response for HTPB/AP propellant at two temperatures.

The coefficients (E, η, m, n) and their ±1 standard deviations from the fitted stress-strain curves of the HTPB/AP propellant in the temperature range from −20 to +60°C are listed in Table 1. The experimental and curve fits for the stress response at two temperatures are shown in Fig. 2. Note that these constitutive models are only valid up to 30–45% strain for predictions above 0°C and 15–20% strain below 0°C. Above these strain levels, bulging of the specimen occurs and its cross-sectional area exceeds the diameter of the input bar of the modified Hopkinson Bar apparatus, resulting in nonuniform stress distribution. Also, extensive crushing and fragmentation of the propellant occurs above these strain levels, as evidenced by photography of the impact event.[3]

In the temperature range from −40 to 40°C, the fitted coefficient for the initial modulus E increases consistently with increasing mean strain rate or decreasing temperature, suggesting that time–temperature superposition is possible for this propellant in the temperature and strain-rate range in this study. This is as expected in filled polymeric composite materials. At 60°C, however, the modulus increased very slightly with temperature, probably due to further crosslinking of the polymeric binder when the temperature approaches the cure temperature (≈55°C).

The fitted value for η is of the same order of magnitude as that estimated from the dynamic shear loss modulus G'' for this propellant, measured by dynamic mechanical thermal analysis[15] at comparable strain rates, supporting the validity of the model. The standard error in the estimated η values, however, is large, and the small difference observed at different temperatures is within the experimental error. Hence, for this study, η is assumed to be independent of temperature, within the temperature range studied here. This is an approximate but valid assumption because the temperature dependence of the viscosity of solid propellants in the temperature range studied here would be expected to be very slight. (An earlier study[7] showed that the HTPB/AP propellant is still ductile at −60°C.) The exponent m is less than one and is consistent with stress softening due to plastic deformation. The exponent n varies between 0.4 and 0.9 and approaches zero at lower temperatures. This is consistent with the propellant being less sensitive to strain rate at lower temperatures because its mechanical behavior is approaching the "glasslike" region.

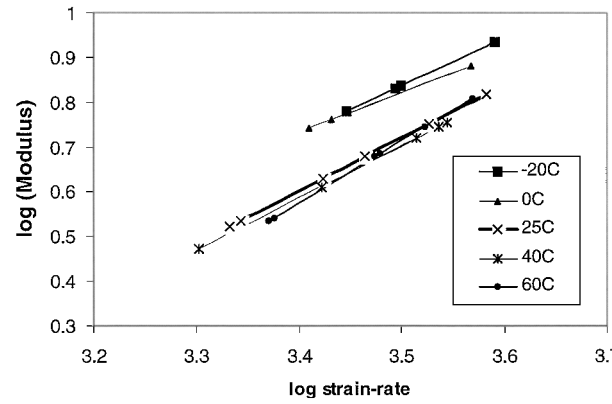

Fig. 3 Modulus vs strain-rate at different temperatures for HTPB/AP propellant.

Time–Temperature Superposition

The results from this and a previous study[7] show that temperature effects under high strain-rate loading can be treated by the conventional approach used in the low strain-rate regime for materials that exhibit thermorheologically simple behavior. According to the time–temperature equivalence principle, increasing (or decreasing) temperature has the same effect on the mechanical property as decreasing (or increasing) strain rate in the temperature range where this assumption is valid. Plots of log E vs log strain rate $\dot{\varepsilon}$ at all five temperatures gave straight lines that are approximately parallel (Fig. 3), indicating a composite or master curve at a reference temperature can be used to represent the data at the other temperatures.

A master curve of log E vs log $(\dot{\varepsilon} a_T)$ was obtained by horizontally superposing the modulus data onto a composite curve using 25°C as the reference temperature (Fig. 4). Here, $\dot{\varepsilon} a_T$ is the reduced strain rate and a_T is the shift factor. The shape of the log a_T vs temperature curve (insert in Fig. 4) can be reasonably fitted to a form that is consistent with applicability of the method of reduced variables. A frequently used representation of the shift factor a_T as a function of temperature for solid propellants is the Williams Landel Ferry (WLF) equation. In this study, the constants, C_1 and C_2, in the WLF equation were determined by fitting the horizontal shift factors to a transformed form of the WLF equation

$$(T - T_0)\log a_T = -C_1(T - T_0) - C_2(\log a_T) \qquad (2)$$

by a multilinear regression analysis and forcing the intercept to pass through zero. The calculated C_1 and C_2 constants for the HTPB/AP propellant, with 25°C as the reference temperature T_0, are 0.03 ± 0.04 and 48 ± 17, respectively. In the calculation of the shift factors, the moduli have not been corrected for the change in thermodynamic reference state[16] because the correction factors were small $[T_0(\mathrm{K})/T(\mathrm{K}) \approx 1$ when $T_0 = 25°\mathrm{C}]$ in the temperature range from T_g (glass transition temperature) to $T_g + 100$. A number of experimental studies[16] suggest that the WLF constants derived for E could also be used for η, that is, the shift factors for E and η were assumed to be similar. In the present study, however, η is assumed to be a constant independent of temperature because it is a relatively small number and the standard errors are large.

Hence, for a given temperature and strain rate, the equivalent stress at a given strain level can be calculated from the master curve,

$$\sigma_R = E_R \varepsilon^m + \eta_R (\dot{\varepsilon} a_T)^n \qquad (3)$$

where E_R is obtained from the master curve (Fig. 4), and η_R, m, and n are the fitted coefficients from the stress–strain curve at the reference temperature (25°C). The shift factor can be calculated from Eq. (2) using the WLF constants. The constitutive equation (3) retains its predictive capability and is reasonable for computational purposes to implement in our finite element code for predicting the structural response of rocket motors.[17]

Evaluation of Mechanical Damage

The stress–strain curves, at 25°C, and fitted coefficients (E, η, m, and n) of Eq. (1) for the PPG/AP propellant with various levels of predamage are shown in Fig. 5 and Table 2, respectively. As expected, the initial modulus E decreases with increasing predamage level, resulting in a reduction in the magnitude of the stress response. The experimental and curve fits of the stress–strain data for predamaged propellants with two different damage levels are shown in Fig. 6.

An approach to incorporate damage into the constitutive law in low strain-rate tests is using a stress correction or softening function to modify the predicted viscoelastic stress response. The softening function g is defined by Swanson et al.[13] as the ratio of the observed stress σ to viscoelastic stress f. Therefore, the stress after correction for damage is given by

$$\sigma = g \cdot f \tag{4}$$

Francis and Thompson[14] modified the original Swanson et al.[13] theory to predict complex loading and unloading solid propellant response. They characterized the softening function from the following simple one-dimensional tests to predict the response from more complex loading histories: 1) constant rate tests at multiple strain rates, 2) a load–unload test, 3) a cyclic loading test, and 4) a simultaneous straining and cooling test. This approach requires extensive testing to calibrate the damage models.

In the present study, an energy approach, based on recoverable strain energy density[18,19] is used to calibrate the softening function g and to assess the level of damage in the propellant specimens before testing on the modified Hopkinson Bar. It is believed that an energy-based approach can predict more adequately the damage in the propellant because it takes into account both the stress and strain capability and is applicable to different loading conditions. Another advantage of this approach is it allows for bulk inelastic behavior, that is, energy dissipated by plastic deformation, etc. The recoverable strain energy density is given by

Table 2 Fit coefficients for stress as a function of strain and strain rate [Eq. (1)] for PPG/AP propellant with various levels of predamage (applied strain energy density); mean strain rate ≈1500 s^{-1}

Induced damage level		$E \pm 1\sigma$,		$\lvert\eta\rvert \pm 1\sigma$,	
W_i, Jm^{-3}	W_{rc}, Jm^{-3}	MPa	$m \pm 1\sigma$	MPa s^{-1}	$n \pm 1\sigma$
0	——	5.6 ± 0.5	0.37 ± 0.02	0.01 ± 0.02	0.6 ± 0.9
2.1×10^3	1.4×10^3	5.8 ± 0.6	0.35 ± 0.02	0.05 ± 1	1 ± 1
2.4×10^3	1.6×10^3	4.4 ± 0.2	0.44 ± 0.01	0.1 ± 0.4	1 ± 1
2.8×10^3	1.8×10^3	5.2 ± 0.2	0.42 ± 0.01	0.1 ± 0.1	0.4 ± 0.3
3.0×10^3	2.0×10^3	4.2 ± 0.5	0.43 ± 0.02	0.1 ± 0.5	1 ± 1

$$W_{rc} = W_i(1 - H_r) \tag{5}$$

where W_i includes the stored energy available for crack growth as well as energy dissipated in viscoelastic processes and plastic deformation. H_r is (loading energy-unloading energy)/loading energy and is a measure of the nonrecoverable energy losses obtained from load–unload experiments.

The calculated recoverable strain energy densities for the PPG/AP specimens with different damage levels are shown in Table 2. The input strain energy density

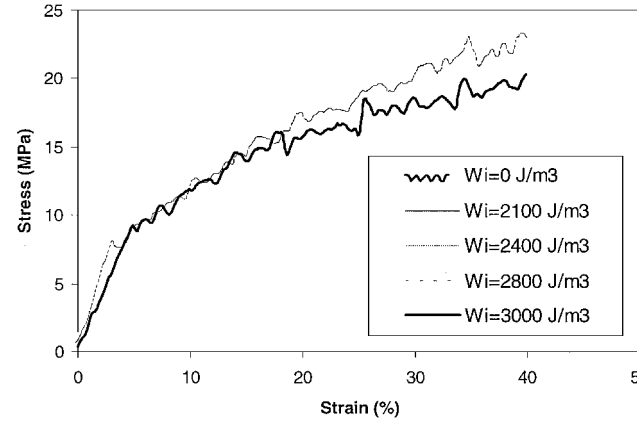

Fig. 5 Stress–strain curves for PPG/AP propellant with various levels of predamage (mean strain rate ≈1500 s^{-1}).

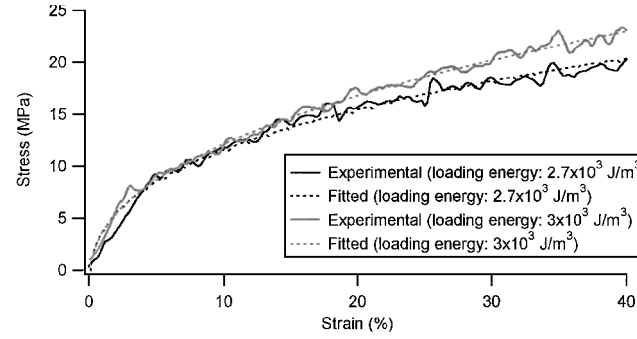

Fig. 6 Comparison between fitted and experimental stress response for predamaged PPG/AP propellant with different damage levels.

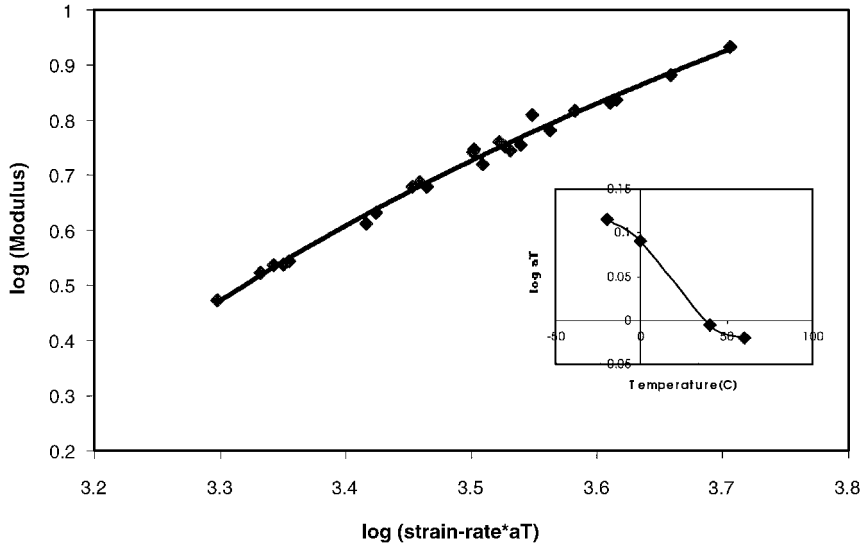

Fig. 4 Master modulus curve and shift factors (inset) vs temperature for HTPB/AP propellant.

$$\int \sigma \, d\varepsilon$$

was calculated from the stress–strain data for the constant stress tests used to induce damage in the specimens. A hysteresis ratio of 0.35 was used for the PPG/AP propellant[18] to calculate W_{rc}. Values of g were determined using Eq. (4), by comparing the observed stresses for the damaged propellant with the stresses predicted from the high strain-rate constitutive model, Eq. (1), for the undamaged propellant.

A function for g, with W_{rc} and $\dot{\varepsilon}$ as the independent variables, was determined by multilinear regression analysis and is given by

$$g = AW_{rc} + B\dot{\varepsilon} + C \tag{6}$$

For the specimen geometry and loading conditions in the present study, this is a piecewise function where

$$g(W_{rc}, \dot{\varepsilon}) = \begin{cases} 1.0 - 6.6 \times 10^{-6} W_{rc} - 48\dot{\varepsilon}, & 0 \le W_{rc} \le 1.8 \times 10^3 \text{ Jm}^{-3} \\ 1.7 - 4.1 \times 10^{-4} W_{rc} + 1.0 \times 10^4 \dot{\varepsilon}, & W_{rc} > 1.8 \times 10^3 \text{ Jm}^{-3} \end{cases}$$

A plot of g vs W_{rc} for tests conducted in the strain-rate range $1–5 \times 10^{-6}$ s^{-1} is shown in Fig. 7. The tests to calibrate the softening functions should be conducted at strain rates representative of the loading conditions that induced the damage in the propellant. The strain rates used here are appropriate to damage induced under rocket motor service life conditions. As shown in Fig. 7, the softening function decreased very markedly with increasing applied strain energy density, above a recoverable strain energy density level of 1.8×10^3 Jm^{-3}, suggestive of two different damage mechanisms. A sufficient amount of predamage is required, that is, the applied strain energy density must exceed a certain level, before the damage is manifested as a reduced stress response in the high strain-rate mechanical properties. The initial decrease in the slope of the g vs W_{rc} plot may be attributed to dewetting and the formation of voids and microcracks. The rapid decrease in the slope once a certain applied strain energy density level is exceeded may be attributed to crack propagation and other secondary deformation processes.

Inclusion of the softening function in the constitutive equation (3) allows damage to be taken into account, as well as temperature and strain-rate dependence:

$$\sigma_D = g\left[E_R \varepsilon^m + \eta_R (\dot{\varepsilon} a_T)^n\right] \tag{7}$$

Here, σ_D is the equivalent stress of the damaged material at the reference temperature. For high strain-rate studies, the parameters in this model can be obtained by curve fitting the stress/strain data from the Hopkinson Bar test at two to three different impact velocities over the temperature range of interest. The softening function g is equal to unity for an undamaged propellant. For damaged propellants, g can be readily calculated from the applied strain energy density and a calibration model, such as Eq. (6).

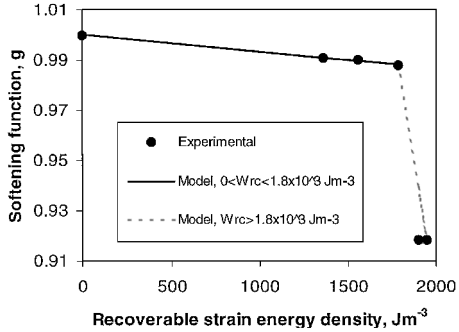

Fig. 7 Stress softening function vs recoverable strain energy density W_{rc} from constant stress tests, strain rates ranging from $1.2e^{-6}$ to $3.5e^{-6}$ s^{-1}.

Stress Predictions

Predamage Induced by Constant Strain-Rate Tests

To test the accuracy of the constitutive equation (7) to predict the response of a PPG/AP propellant that was damaged by different loading conditions, the specimen was predamaged by a monotonic loading test at constant strain rate ($\approx 10^{-5}$ s^{-1}) until failure, before testing on the modified Hopkinson Bar.

The softening function for the damaged propellant was calculated from the recoverable strain-energy density and strain rate of the monotonic test using Eq. (6). A comparison between the measured and predicted stress response is shown in Fig. 8. The model predicts the stress response quite well, up to the maximum strain level ($\approx$30% for this propellant). Above this strain level, extensive deformation, cracking, and fragmentation of the propellant occurred.

Effect of Temperature

The constitutive equation (7) was also used to predict the response of a HTPB/AP propellant at −40 and −50°C, which are outside the temperature range used to develop the model, but inside the range of the reduced strain rate $\dot{\varepsilon} a_T$. By the use of the mean

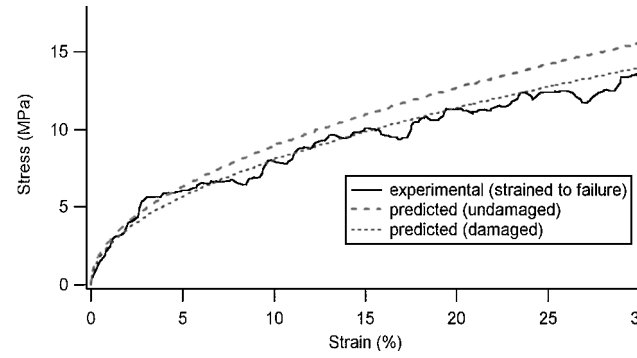

Fig. 8 High strain-rate nonlinear viscoelastic stress prediction for PPG/AP propellant predamaged by straining to failure under monotonic constant strain-rate test.

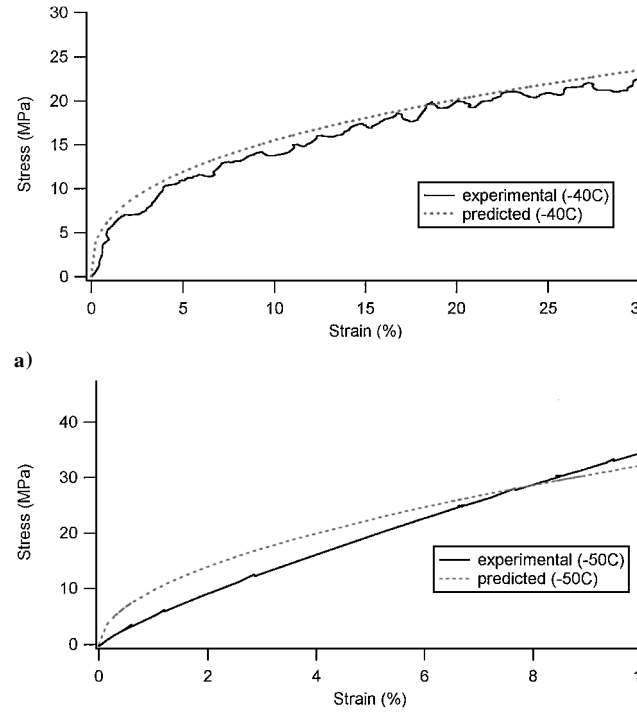

Fig. 9 High strain-rate viscoelastic stress prediction for HTPB/AP propellant at a) − 40°C (mean strain rate $\approx$2300 s^{-1}) and b) − 50°C (mean strain rate $\approx$4300 s^{-1}).

strain rate of the experiments at these temperatures, the mean E_R was estimated from the plot of log E_R vs log $\dot{\varepsilon} a_T$ using a third-order polynomial fit (Fig. 4). A comparison of the predicted stress response at -40 and -50°C and the measured data are given in Figs. 9a and 9b. The reasonable comparison (2–60% difference between the predicted and measured data) suggests the validity of the time–temperature superposition principle for high strain rates and the ability of the model to predict outside the measured temperature range, within the extended temperature–strain rate range of the analysis.

Conclusions

The prediction of the high strain-rate mechanical behavior of NLVE materials, such as solid rocket propellants, has been the subject of the present study. A stress softening function was used to modify the viscoelastic function, derived from a semi-empirical fit of high strain-rate data from the modified Hopkinson Bar test, accounting for damage effects. The numerical parameters in this model could be related to the physics of the propellant, that is, modulus in the initial linear elastic region, pseudoviscosity, and the exponents describing strain softening/hardening and strain-rate sensitivity. A continuum energy-balanced approach, using the recoverable strain energy density to quantify the amount of damage, was utilized to calibrate the stress softening function. The time-temperature superposition principle was used to modify the constitutive model, accounting for the effects of loading variables such as temperature and strain rate.

The stress response predicted by the constitutive model was compared with experimental data for two different solid composite propellants under different loading conditions. The model can predict the stress response up to 15–40% strain (depending on the temperature). Above this strain level, extensive bulging, cracking, and fragmentation of the propellant occurs. The reasonably good correlation between the predicted and experimental stress response indicate that, first, within the appropriate temperature and strain-rate ranges, the constitutive equation (3) can be used for temperature–strain rate conversion. Second, a stress softening function, characterized from simple tests that is based on an energy approach and varies with recoverable strain energy density and strain rate can successfully predict damage under high strain-rate loading conditions. The present method to incorporate damage in the viscoelastic functions necessitates separate tests to characterize the softening functions and the viscoelastic parameters. The viscoelastic losses are time dependent, but recoverable. On the other hand, the softening function is a measure of the nonrecoverable energy attributed to dewetting, formation of voids/microcracks, and crack propagation. A microstructural constitutive theory may be required to link/unify these different phenomena in a single model.

It is planned to implement these models into our finite element structural analysis code[17] to predict propellant fracture and deformation response to high strain-rate impact loading in rocket motors.

References

[1]Dienes, J. K., and Kershner, J. D., "Multiple Shock Initiation via Statistical Crack Mechanics," *Proceedings of the 11th International Detonation Symposium*, Publication ONR333000-5, 1998, pp. 717–724.

[2]Winter, R. E., and Field, J. E., "The Role of Localized Plastic Flow in the Impact Initiation of Explosives," *Proceedings of the Royal Society of London, Series A: Mathematical and Physical Sciences*, Vol. 343, 1975, pp. 399–413.

[3]Ho, S.-Y., "Impact Ignition Mechanisms of Rocket Propellants," *Combustion and Flame*, Vol. 91, 1992, pp. 131–142.

[4]Green, L. G., James, E., Lee, E. L., Chambers, E. S., Tarver, C. M., Westmorland, C., Weston, A. M., and Brown, B., "Delayed Detonation in Propellants from Velocity Impact," *Proceedings of the 7th International Detonation Symposium*, 1981, pp. 256–264.

[5]Francis, E. C., Peters, R. L., and Huffred, W. L., "Considerations in the Applications of Non-Linear Structural Materials," *Proceedings of 2nd International Conference on Mechanical Behaviour of Materials*, 1976.

[6]Mullins, L., "Softening of Rubber by Deformation," *Rubber Chem and Technology*, Vol. 31, 1969, pp. 333–362.

[7]Ho, S.-Y., and Fong, C. W., "Temperature Dependence of High Strain-Rate Impact Fracture Behaviour in Highly Filled Polymeric Composite and Plasticized Thermoplastic Propellants," *Journal of Materials Science*, Vol. 22, 1987, pp. 3023–3031.

[8]Ho, S.-Y., "High Strain-Rate Impact Studies of Pre-damaged Rocket Propellants, I. Characterisation of Damage Using a Cumulative Damage Failure Criterion," *Combustion and Flame*, Vol. 104, 1996, pp. 524–534.

[9]Little, R. R., and Rice, J. R., "Investigating Damage in Composite Solid Propellants," *Proceedings of the JANNAF Structures and Mechanical Behaviour Subcommittee Meeting* (to be published).

[10]Wulf, G. T., and Richardson, G. T., "The Measurement of Dynamic Stress–Strain Relationships at Very High Strains," *Journal of Physics E: Scientific Instruments*, Vol. 7, 1973, pp. 167–169.

[11]Ho, S.-Y., Fong, C. W., and Hamshere, B. L., "Assessment of Response of Rocket Propellants to High Velocity Projectile Impact Using Small-Scale Laboratory Tests," *Combustion and Flame*, Vol. 77, 1989, pp. 395–404.

[12]Ho, S.-Y., and Fong, C. W., "Relationship Between Impact Ignition Sensitivity and Kinetics of the Thermal Decomposition of Solid Propellants," *Combustion and Flame*, Vol. 75, 1989, pp. 139–151.

[13]Swanson, S. R., Christensen, L. W., and Christensen, R. J., "A Constitutive Formulation for High Elongation Propellant," *Journal of Spacecraft and Rockets*, Vol. 20, No. 6, 1983, pp. 559–566.

[14]Francis, E. C., and Thompson, R. E., "Nonlinear Structural Modeling of Solid Propellants," *Proceedings of the AIAA/SAE/ASME Joint Propulsion Conference*, AIAA, New York, 1984, pp. 1–5.

[15]Ho, S.-Y., "Viscoelastic Response of Solid Rocket Motor Components for Service Life Assessment," *Journal of Materials Science*, Vol. 32, No. 19, 1997, pp. 5155–5161.

[16]Ferry, J. D., *Viscoelastic Properties of Polymers*, 3rd ed., Wiley, New York, 1980.

[17]Ho, S.-Y., and Carè, G., "Modified Fracture Mechanics Approach in Structural Analysis of Solid-Rocket Motors," *Journal of Propulsion and Power*, Vol. 14, No. 4, 1998, pp. 409–415.

[18]Ho, S.-Y., and Tod, D. A., "Mechanical Failure Analysis of Rubbery Composite Propellants Using a Modified Fracture Mechanics Approach," *Proceedings of the 21st International Conference of ICT*, 1990, pp. 1–14.

[19]Kinloch, A. J., and Tod, D. A., "A New Approach to Crack Growth in Rubbery Composite Propellants," *Propellants Explosives and Pyrotechnics*, Vol. 9, 1984, pp. 48–55.